


**Possible wobbling phenomenon in  $^{125}\text{Xe}$** Mamta Prajapati  and Somnath Nag *Department of Physics, Indian Institute of Technology (BHU) Varanasi 221005, India*

A. K. Singh

*Department of Physics, Indian Institute of Technology Kharagpur, West Bengal 721302, India*

A. Al-Khatib

*Department of Physics, Faculty of Science, University of Damascus, Damascus, Syria*H. Hübel  and A. Neußer-Neffgen<sup>†</sup>*Helmholtz–Institut für Strahlen- und Kernphysik, Universität Bonn, Nußallee 14-16, D-53115 Bonn, Germany*G. B. Hagemann, G. Sletten, and B. Herskind<sup>‡</sup>*Niels Bohr Institute, Blegdamsvej 17, DK-2100 Copenhagen, Denmark*C. R. Hansen *Department of Clinical Research, University of Southern Denmark, Odense, Denmark  
and Department of Oncology, Odense University Hospital, Odense, Denmark*G. Benzoni  and A. Bracco*Dipartimento di Fisica, Universitè'a di Milano and INFN, I-20133 Milano, Italy*R. V. F. Janssens *Department of Physics and Astronomy, University of North Carolina at Chapel Hill, Chapel Hill, North Carolina 27599, USA  
and Triangle Universities Nuclear Laboratory, Duke University, Durham, North Carolina 27708, USA*

M. P. Carpenter

*Physics Division, Argonne National Laboratory, Argonne, Illinois 60439, USA*

P. Chowdhury

*Department of Physics, University of Massachusetts Lowell, Lowell, Massachusetts 01854, USA*

(Received 22 September 2023; accepted 12 December 2023; published 1 March 2024)

In the present paper, negative-parity bands based on the  $\nu h_{11/2}$  configuration in  $^{125}\text{Xe}$  have been revisited. This nucleus was populated through the reaction  $^{82}\text{Se}(^{48}\text{Ca}, 5n)^{125}\text{Xe}$  at a beam energy of 205 MeV and the corresponding  $\gamma$  rays were observed using the Gammasphere spectrometer. Evidence for first and second phonon wobbling excitations has been established by measurements of directional correlation ratios and angular distributions of the involved  $\gamma$  rays. The observed wobbling energy of the bands involved were compared with the recently published results obtained within the framework of triaxial projected shell-model calculations.

DOI: [10.1103/PhysRevC.109.034301](https://doi.org/10.1103/PhysRevC.109.034301)**I. INTRODUCTION**

A nucleus with a stable triaxial shape exhibits different moments of inertia associated with the intermediate (m), long (l),

and short (s) axes ( $\mathfrak{I}_m > \mathfrak{I}_l \neq \mathfrak{I}_s$ ), respectively. Therefore, the quantal rotation of such a nucleus about either of the three principal axes no longer remains equivalent. The concept of triaxiality has been invoked to explain anomalous signature splittings and signature inversions in odd- $A$  nuclei. Experimentally triaxiality at moderate and high spin can be realized either through wobbling motion, chiral symmetry breaking, or through the presence of a  $\gamma$  band [1–4].

Bohr and Mottelson anticipated the wobbling motion of a triaxial even-even nucleus for the first time [1]. The triaxial

\*somnathn.phy@itbhu.ac.in

<sup>†</sup>Present address: Wagner & Albiger Patent Attorneys, Siegfried-Leopold-Straße 27, 53225 Bonn, Germany.<sup>‡</sup>Deceased.

nucleus favors rotation about an axis that generates the largest moment of inertia, which corresponds to the minimum energy of the system. However, at a slightly higher energy, the same axis may execute a quantized harmonic oscillation about a space-fixed angular momentum axis. This results in distinct rotational bands corresponding to the different oscillation quanta, known as wobbling phonons labeled by the number  $n_\omega$ .

In odd- $A$  nuclei, the wobbling phenomena are classified as being longitudinal wobbling (LW) and transverse wobbling (TW) based on the way the angular momentum of the odd quasiparticle couples to that of the core (for more details see Ref. [3]). Generally speaking, in odd- $A$  nuclei, in addition to the  $n_\omega = 1$  wobbling band, there exists a signature partner band to the  $n_\omega = 0$  yrast band with the same signature. This signature partner (SP) band occurs both in axial and triaxial nuclei. One distinguishing feature of the wobbling phenomenon, compared to a signature partner band in a triaxial nucleus, is the presence of  $\Delta I = 1$   $\gamma$ -ray transitions with large  $E2$  admixtures between the successive wobbling bands [3,5].

The Xe ( $Z = 54$ ) nuclei lie in a transitional region between spherical Sn ( $Z = 50$ ) and deformed Ce ( $Z = 58$ ) nuclei. This leads to a fragile coexistence of deformation-dependent excitation modes. In odd-mass Xe nuclei, the unique negative-parity  $h_{11/2}$  neutron orbitals form the yrast rotational bands and their signature splitting features are well described by theoretical model calculations [6–8]. In addition, the second negative-parity rotational bands based on the  $h_{11/2}$  neutron orbital (called the yrare bands) have also been observed. However, in contrast to the yrast band, the parameter

$$S(I) = [E(I) - E(I - 1)]/2I \quad (1)$$

which is used to visualize the signature splitting is inverted in the yrare ones [9]. The magnitude of  $S(I)$  depends on the projection of the total angular momentum on the symmetry axis (the  $K$  quantum number). However, nonconservation of  $K$  in triaxial nuclei leads to different  $K$  mixing in the corresponding structures and, hence, the signature splitting may appear different [11]. Thus, the quantity  $S(I)$  is found to be an effective tool to quantify the degree of triaxiality in atomic nuclei [12]. Since, for the Xe isotopes, triaxial shapes have been suggested [11], Moon *et al.* [9] addressed the existence of signature inversion with small splitting in the yrare bands of  $^{125}\text{Xe}$ . In their work, bands 1 and 3 (as shown in Fig. 1) were reported as favored and unfavored signature partners having a large signature splitting. On the other hand, bands 2 and 4 were suggested to be yrare bands with small signature splitting, where the variation of  $S(I)$  as a function of  $I$  is inverted with respect to that of the yrast bands. They concluded that the yrast bands originate from a  $\nu h_{11/2}$  [532]7/2 configuration, whereas, owing to a comparatively large signature splitting between  $\alpha = \pm 1/2$  states across the [535]5/2 configuration the yrare states could not be explained with a second  $h_{11/2}$  orbital. Instead, the yrare bands may be associated with the coupling of a  $\gamma$  phonon to the  $h_{11/2}$  neutron. According to Hamamoto [13], such signature inversion can occur in a nucleus with a triaxial shape when the angular momentum of the collective rotation in the unfavored-signature states points in

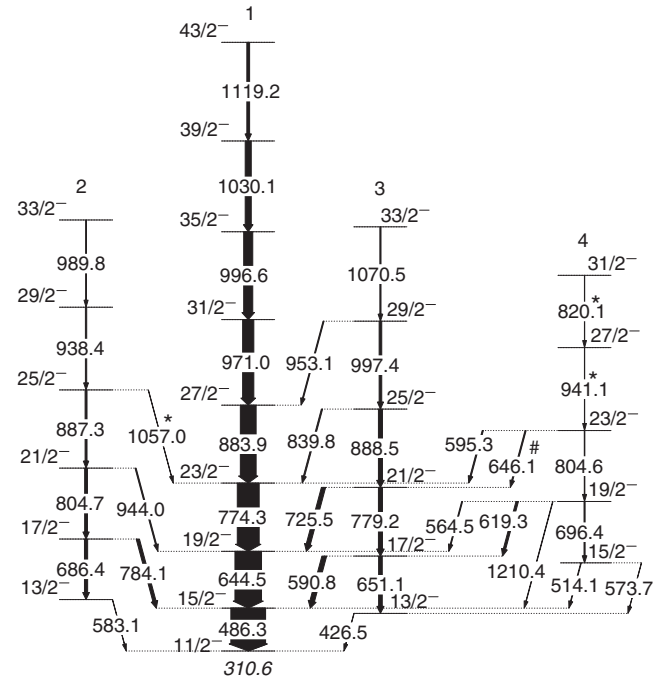


FIG. 1. Partial level scheme of  $^{125}\text{Xe}$  which is mostly based on earlier works by Al-Khatib *et al.* and Moon *et al.* [9,28]. The transitions shown with “\*” are taken from [9] as these transitions were very weak in our data. Only one new  $\gamma$  transition is shown with “#”. To avoid contamination, the centroid of each transition was determined by gating on the nearest neighbor  $\gamma$  ray. The intensities of transitions in band 1 have been measured in the gate on the 486.3-keV  $\gamma$  ray while normalizing with respect to the intensity of the 644.5-keV one. Similarly, the intensities of transitions in bands 2, 3, and 4 were determined by gating on respective decay-out transitions. The width of each transition represents the normalized intensity of the corresponding transitions. Measurement of normalized intensity was not possible for the transitions with “\*” and energies 426.5, 583.1, and 573.7 keV and hence the said transitions are shown in the level scheme by arrows having width 1.0. For more details see the Supplemental Material [10].

a direction that is different from the one specified by the large moment of inertia for a certain triaxial intrinsic shape. However, the mass-dependent  $S(I)$  values of the quasi- $\gamma$  bands in even Xe isotopes are not inverted [14]. Therefore, it may not be entirely appropriate to examine the evolution of the yrare bands using such a simplistic coupling scheme.

In recent years, this type of unfavored signature partner bands based on the  $\nu h_{11/2}$ ,  $\pi h_{11/2}$ , and  $\pi i_{13/2}$  configurations have been revisited in  $^{127}\text{Xe}$  [14],  $^{133}\text{La}$  [15],  $^{183}\text{Au}$  [16], and it was observed that these can be described by wobbling with the presence of enhanced  $\Delta I = 1$ ,  $E2$  transitions. In comparison to other mass regions, this phenomenon has been observed near  $A \approx 130$  at a lower value of the deformation ( $\epsilon \approx 0.16$ ) [14,15,17].

The  $^{125}\text{Xe}$  nucleus is the nearest odd- $A$  neighbor to  $^{127}\text{Xe}$ , which along with  $^{133}\text{La}$ , is known to exhibit longitudinal wobbling [14,15]. All other isotopes, i.e.,  $^{161,163,165,167}\text{Lu}$  [18–21],  $^{135}\text{Pr}$  [22,23],  $^{133}\text{Ba}$  [17],  $^{105}\text{Pa}$  [24],  $^{183}\text{Au}$  [16], exhibit transverse wobbling motion. The transverse wobbling charac-

teristics proposed in some of the nuclei are debatable [25]. In a recent publication on  $^{131}\text{Xe}$  by Chakraborty *et al.*, [26], the authors concluded that odd- $A$  nuclei, where a wobbling band has been observed, are mostly surrounded by two even-even nuclei with  $R_E \geq 2.3$  and  $Q_0 \geq 2.6$  b (where  $R_E = E_{4^+}/E_{2^+}$  is the ratio of the energies of the first  $2^+$  and  $4^+$  levels and  $Q_0$  is the intrinsic quadrupole moment.  $Q_0 = 2.6$  b corresponds to  $\varepsilon = 0.16$ ). The same is true for  $^{127}\text{Xe}$ . The nucleus  $^{125}\text{Xe}$  is surrounded by  $^{124}\text{Xe}$  which has  $R_E = 2.48$ ,  $Q_0 = 3.28$  b and  $^{126}\text{Xe}$  with  $R_E = 2.42$ ,  $Q_0 = 2.8$  b. It is to be noted that, as per Casten's symmetry triangle,  $R_E = 2.5$  corresponds to  $\gamma$ -soft [O(6)] nuclei [27]. Thus, the magnitude of  $R_E$  and  $Q_0$  in the neighboring even-even nuclei also makes  $^{125}\text{Xe}$  a suitable candidate to search for wobbling motion. In the present work, the partial level scheme of  $^{125}\text{Xe}$  has been studied with the main aim to measure mixing ratios of the  $\Delta I = 1$  inter-band transitions and determine  $E2$  admixtures in these transitions as these represent an important fingerprint for wobbling.

## II. EXPERIMENTAL DETAILS

The detailed description of the experiment was published in Ref. [28] and is only briefly summarized here. Excited states of  $^{125}\text{Xe}$  were populated in the reaction  $^{82}\text{Se}(^{48}\text{Ca}, 5n)^{125}\text{Xe}$  at a beam energy of 205 MeV using the ATLAS accelerator at Argonne National Laboratory. Details on the target are given in Ref. [29]. The de-exciting  $\gamma$  rays were detected with the Gammasphere array [30]. A total of  $2.8 \times 10^9$  events with coincidence fold  $\geq 5$  were collected. The coincidence data were stored in  $\gamma$ - $\gamma$  matrices, a  $\gamma$ - $\gamma$ - $\gamma$  cube, and a  $\gamma^4$  hypercube. The RADWARE package [31] was used in the analysis of coincidence relationships. Two asymmetric matrices were constructed to determine the multiplicities of the  $\gamma$  rays, based on the directional correlation of oriented nuclei ratios (DCO ratios). The first matrix includes the events detected in forward and backward ( $fb$ ) detectors at an average angles of  $35^\circ$  and  $145^\circ$  on one axis, and those detected at near to  $\approx 90^\circ$  on the other, whereas the second matrix consists of events registered in detectors near to  $\approx 90^\circ$  on one axis with those detected at an average angles of  $35^\circ$  and  $145^\circ$  on the other. The DCO ratio [28] is defined as

$$R_{\text{DCO}} = \frac{I_{\gamma_1 \text{ at } fb, \text{ gated by } \gamma_2 \text{ at } \approx 90^\circ}}{I_{\gamma_2 \text{ at } \approx 90^\circ, \text{ gated by } \gamma_1 \text{ at } fb}}. \quad (2)$$

To measure the angular distribution of the  $\gamma$  rays, intensity of  $\gamma$  photons is measured across detectors placed along average angles of  $35^\circ$ ,  $50^\circ$ ,  $70^\circ$ ,  $80^\circ$ ,  $90^\circ$ ,  $100^\circ$ ,  $110^\circ$ ,  $130^\circ$ ,  $145^\circ$ , and  $163^\circ$  angles with respect to the beam direction. Efficiency correction was performed at each angle by using  $^{182}\text{Ta}$ ,  $^{88}\text{Y}$ , and  $^{207}\text{Bi}$  standard calibration sources.

## III. DATA ANALYSIS AND RESULTS

In the previous work, excited states in the negative-parity bands of  $^{125}\text{Xe}$  were studied [9,28,32,33]. However, no clear theoretical explanation was provided for these bands. The current study focuses on the measurement of mixing ratios of inter-band transitions at low spin, which are essential for analyzing the wobbling mode. To investigate the nature of  $\Delta I = 1$  transitions decaying from band 3 to band 1, the DCO

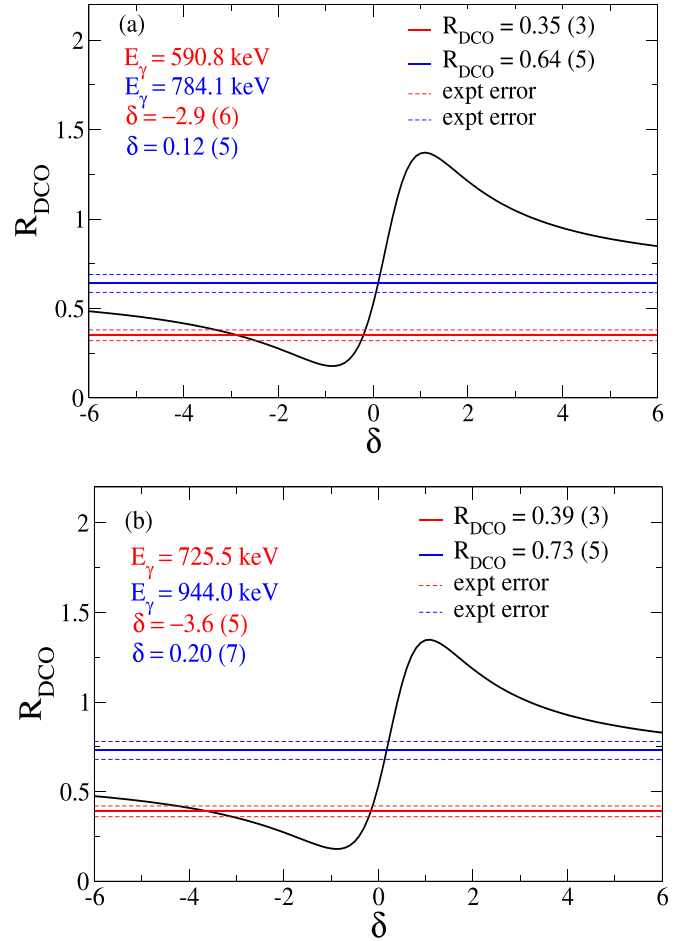


FIG. 2. Variation of the theoretical  $R_{\text{DCO}}$  value (black line) as a function of the mixing ratio  $\delta$  plotted for different  $\Delta I = 1$  transitions. The red lines correspond to the experimental value of  $R_{\text{DCO}}$  for the (a) 590.8- and (b) 725.5-keV transitions decaying from band 3 to band 1. The blue lines correspond to the experimental value of  $R_{\text{DCO}}$  for the (a) 784.1- and (b) 944.0-keV transitions decaying from band 2 to band 1.

ratios of these transitions were first determined. When the gating transition is of stretched quadrupole nature, the  $R_{\text{DCO}}$  value is  $\approx 1.0$  for stretched quadrupole transitions and  $\approx 0.6$  for stretched dipole ones. These ratios agree well with the assignments by Granderath *et al.* [32]. The value of the  $R_{\text{DCO}}$  depends on the detector geometry as well as on the sub-state population width, ( $\sigma/j$ ), achieved in the fusion evaporation reaction. To calculate this width, the theoretical values of  $R_{\text{DCO}}$  were calculated with the ANGCOR code [34] and were compared with the experimental values for dipole transitions at different values of  $\sigma/j$  by varying the mixing ratio ( $\delta$ ). The comparison between the theoretical and experimentally observed  $R_{\text{DCO}}$  ratios suggests that the value of  $\sigma/j$  is  $\approx 0.30$ .

The  $R_{\text{DCO}}$  values connecting  $\Delta I = 1$  transitions are nearly equal to those obtained by Granderath *et al.* [32] and these do not match with the typical values expected for dipole transitions, herewith suggesting strong mixing. In Fig. 2(a), the theoretical  $R_{\text{DCO}}$  values are plotted as a function of  $\delta$  for the 784.1- and 590.8-keV transitions ( $17/2^- \rightarrow 15/2^-$ ,  $\Delta I = 1$ ). The  $15/2^- \rightarrow 11/2^-$ ,  $\Delta I = 2$  transition with energy of 486.3

TABLE I. List of the energies of the  $\gamma$  transitions, spins, experimental  $a_2$ - $a_4$  values,  $R_{DCO}$  values, mixing ratios ( $\delta_{E2/M1}$ ), E2 fractions ( $= \frac{\delta^2}{1+\delta^2}$ ) and transition probability ratios for corresponding  $\Delta I = 2$  intra- and  $\Delta I = 1$  inter-band  $\gamma$ -ray transitions of  $^{125}\text{Xe}$ .

$E_\gamma$ (keV)	$I_i \rightarrow I_f$	$a_2$	$a_4$	$R_{DCO}$	$\delta_{E2/M1}^a$	E2%	$\frac{B(E2_{out})}{B(E2_{in})}$	$\frac{B(M1_{out})}{B(E2_{in}^2)}$ $(\frac{\mu_N}{e^2 b^2})$
590.8	$17/2^- \rightarrow 15/2^-$	$-0.72$ (2)	$0.19$ (4)	$0.35$ (3)	$-1.94^{+20}_{-21}$	$79\%^{+3\%}_{-4\%}$	$1.60$ (17)	$0.10$ (2)
725.5	$21/2^- \rightarrow 19/2^-$	$-0.68$ (3)	$0.17$ (4)	$0.39$ (3)	$-2.12^{+27}_{-22}$	$81.8\%^{+33\%}_{-35\%}$	$1.19$ (12)	$0.09$ (2)
839.8	$25/2^- \rightarrow 23/2^-$	$-0.64$ (3)	$0.20$ (4)	$0.40$ (3)	$-2.40^{+28}_{-26}$	$85.2\%^{+25\%}_{-33\%}$	$0.33$ (5)	$0.028$ (5)
619.3	$19/2^- \rightarrow 17/2^-$	$-0.56$ (3)	$0.21$ (4)	$0.46$ (4)	$-2.81^{+36}_{-34}$	$88.7\%^{+23\%}_{-28\%}$	$3.57$ (54)	$0.12$ (3)
784.1	$17/2^- \rightarrow 15/2^-$	$-0.23$ (3)	$0.03$ (5)	$0.64$ (5)	$0.32^{+6}_{-4}$	$9.3\%^{+26\%}_{-21\%}$	$0.045$ (12)	$0.190$ (15)
944.0	$21/2^- \rightarrow 19/2^-$	—	—	$0.73$ (5)	—	—	—	—

<sup>a</sup>mixing ratio obtained from angular distribution method from the present study.

keV was employed as the gating one. The value of  $\delta$  extracted for the 784.1-keV transition is 0.12 (5) and that for the 590.8-keV one, it is  $-2.9$  (6). Similarly, in Fig. 2(b), the  $\delta$  values

for the 944.0- and 725.5-keV transitions are calculated. The experimental values of  $R_{DCO}$  for interband  $\Delta I = 1$  transitions are summarized in Table I. The large values of  $\delta$  for the 590.8-

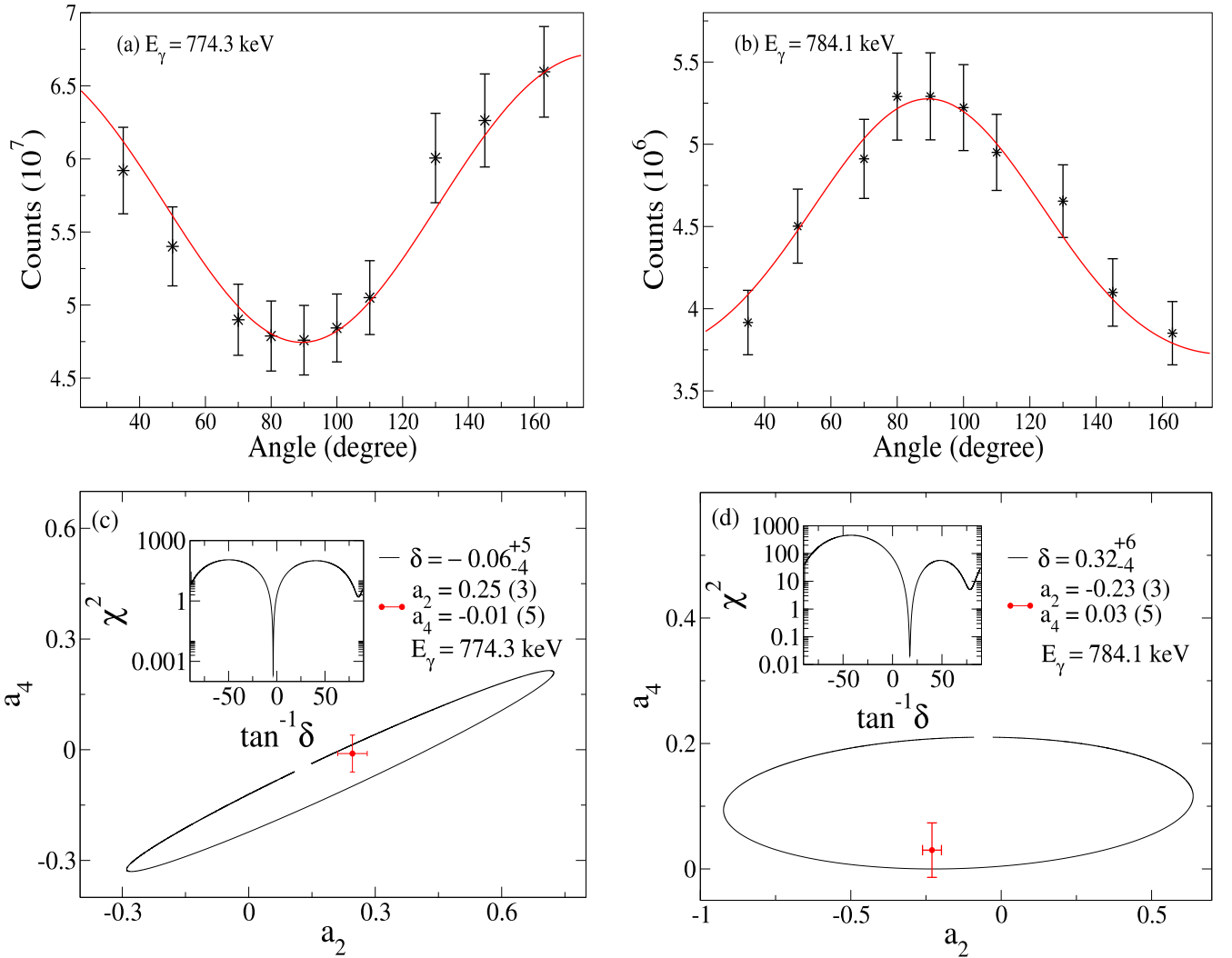


FIG. 3. (a) and (b) represent the angular distribution plots for the 774.3-keV  $\gamma$  ray (quadrupole transition) and the 784.1-keV  $\gamma$  ray (dipole transition) determined with a coincidence gate on 486.3-keV (quadrupole transition)  $\gamma$  ray. (c) and (d) represent the  $a_2$ - $a_4$  contour plots for the 774.3- and 784.1-keV transitions, respectively. The inset provides the  $\chi^2$  analysis for the experimental angular distribution of the corresponding transitions.

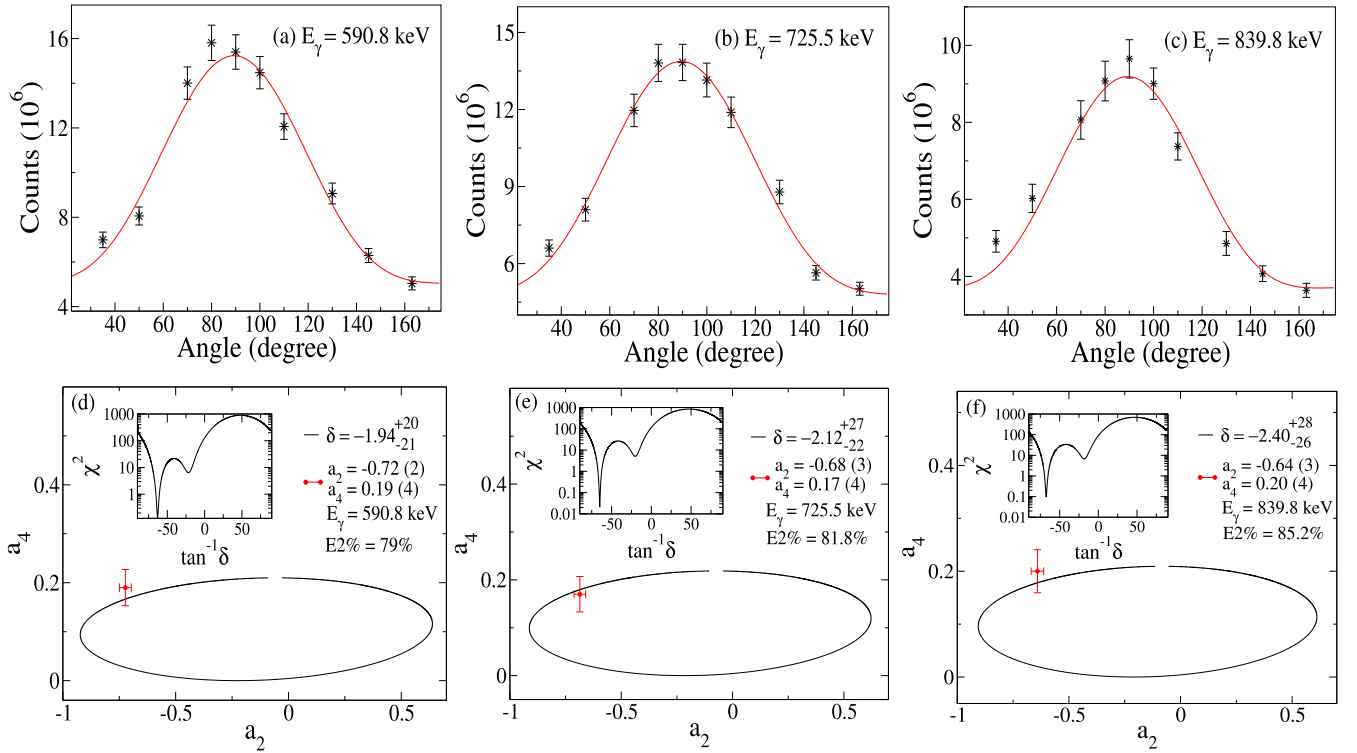


FIG. 4. (a), (b), and (c) represent the angular distributions for the 590.8-, 725.5-, and 839.8-keV ( $\Delta I = 1$ ) transitions with a coincidence gate placed on the 486.3-keV  $\gamma$  ray. The  $a_2$ - $a_4$  contour plots of the 590.8-, 725.5-, and 839.8-keV transitions are shown in the lower panels (d), (e), and (f). The corresponding  $\chi^2$  minimization is displayed in the insets.

725.5-, and 839.8-keV transitions (from band 3 to band 1) indicate that they are characterized by large  $E2$  admixtures.

Furthermore, the arrangement of around five to ten Compton-suppressed Ge detectors across different mentioned angles of the Gammasphere array provides an opportunity for high-statistics angular distribution measurements. The angular distribution of  $\gamma$  rays is given by the usual expression

$$W(\theta) = A_0[1 + a_2(P_2 \cos \theta) + a_4(P_4 \cos \theta)], \quad (3)$$

where  $a_2$ ,  $a_4$  are angular distribution coefficients and  $P_2(\cos \theta)$  and  $P_4(\cos \theta)$  are Legendre polynomials. The validity of the method has been established by examining the angular distribution for known stretched- $E2$  and  $M1$  transitions (774.3- and 784.1-keV  $\gamma$  rays, respectively). The mixing ratios extracted for these two transitions are very small (see Fig. 3).

Supporting the proposed assignments, the angular distribution plots for the 590.8-, 725.5-, and 839.8-keV interband transitions are depicted in Figs. 4(a), 4(b), and 4(c), respectively. The  $a_2$ - $a_4$  contour plots, along with the experimentally extracted values for these transitions, are displayed in Figs. 4(d), 4(e), and 4(f). It can be seen that the interband  $\Delta I = 1$   $\gamma$ -ray transitions between bands 1 and 3 are characterized by large  $E2$  admixtures, up to 85.2% (see Fig. 5).

Similarly, the angular distribution plot for the 619.3-keV transition and the corresponding  $a_2$ - $a_4$  contour are shown in Figs. 6(a) and 6(b), respectively. The observed  $E2$  admixture for this transition is 88.7%, which is slightly larger than that of the  $\Delta I = 1$   $\gamma$ -ray transitions from band 3 to band 1.

Decay transitions have also been observed from band 4 to bands 3 and 1 with  $\Delta I = 1, 2$ , respectively. A similar pattern has been observed in  $^{163}\text{Lu}$  [35],  $^{165}\text{Lu}$  [20], and  $^{135}\text{Pr}$  [23]. Furthermore,  $\Delta I = 0$  transitions have also been found in  $^{125}\text{Xe}$  which link bands 4 and 1. A similar observation was reported in  $^{127}\text{Xe}$  [14] and  $^{133}\text{Ba}$  [17]. A coupling between a  $\gamma$  vibration and the wobbling motion was suggested to account for these observations.

To determine the  $E2$  character of the linking transitions, the transition probability ratios  $B(E2_{\text{out}})/B(E2_{\text{in}})$  were measured. These ratios, with their corresponding mixing ratios and  $E2$

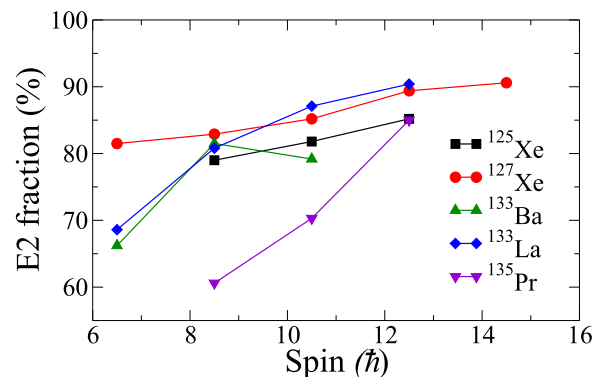


FIG. 5.  $E2$  fraction with respect to spin for  $\Delta I = 1$   $\gamma$ -ray transitions between  $n_w = 1$  and  $n_w = 0$  wobbling bands in different nuclei in the low spin regime.



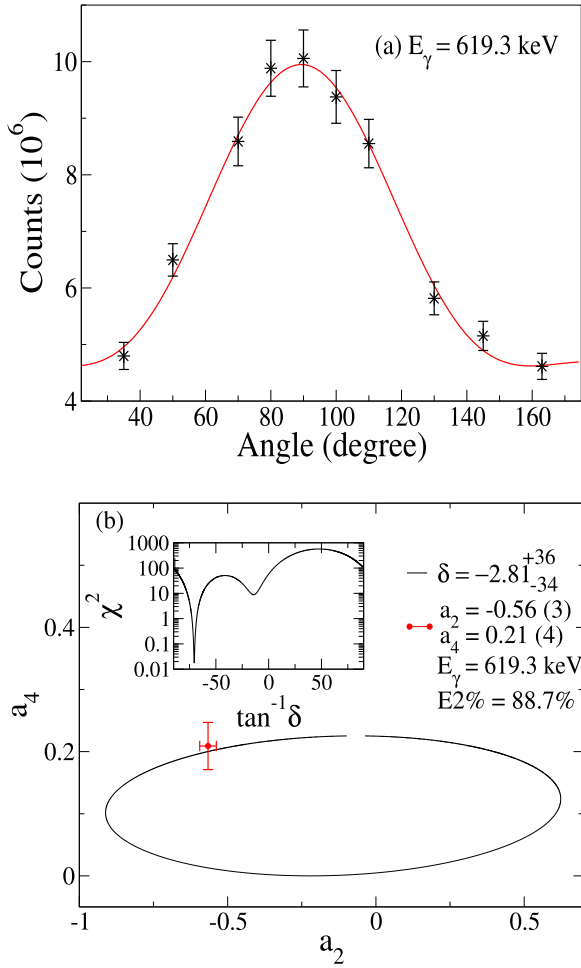


FIG. 6. (a) and (b) represent the angular distribution and  $a_2$ – $a_4$  contour plot for the 619.3-keV transition with a coincidence gate on the 486.3-keV  $\gamma$  ray.

fractions, are summarized in Table I. Small  $B(M1_{out})/B(E2_{in})$  values were obtained, as expected for wobbling phonon bands, owing to large  $E2$  transition probabilities. The large  $B(E2_{out})/B(E2_{in})$  values also support the predominant  $E2$  character of the linking transitions [2,14–17]. The wobbling energy  $E_{wobb}$  [3] is defined as

$$E_{wobb} = E(I, n_\omega = 1) - \frac{E(I-1, n_\omega = 0) + E(I+1, n_\omega = 0)}{2} \quad (4)$$

and is calculated here from the level energies of bands 1 and 3 in  $^{125}\text{Xe}$ . In Fig. 7,  $E_{wobb}$  values have been plotted for different wobblers nuclei along with those for  $^{125}\text{Xe}$ . This  $E_{wobb}$  value increases with spin for the  $^{133}\text{La}$  [15],  $^{127}\text{Xe}$  [14], and  $^{125}\text{Xe}$  nuclei, whereas it gradually decreases for  $^{133}\text{Ba}$  [17] and  $^{135}\text{Pr}$  [22,23]. It is well known that longitudinal wobbling is characterized by wobbling energy increasing with angular momentum, whereas for transverse wobbling,  $E_{wobb}$  decreases with increasing angular momentum [3]. Thus, the wobbling motion in  $^{125}\text{Xe}$  can be categorized as being longitudinal. This may be due to the alignment of quasineutrons along the

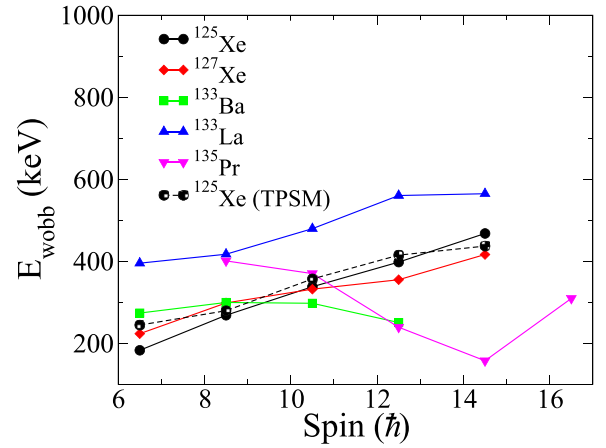


FIG. 7. Experimentally observed  $E_{wobb}$  energies with respect to spin for  $^{133}\text{La}$  [15],  $^{127}\text{Xe}$  [14],  $^{133}\text{Ba}$  [17],  $^{135}\text{Pr}$  [22,23],  $^{125}\text{Xe}$  (this work and TPSM result).

middle axis of the triaxial core. A similar argument was given for longitudinal wobbling in  $^{127}\text{Xe}$  [14].

Band 2 has the same signature quantum number as band 3, but has higher excitation energies (see Fig. 8). This is expected for an unfavored signature partner band of  $n_\omega = 0$ . One of the important characteristics of the signature partner band is the occurrence of  $\Delta I = 1$ ,  $M1$  transitions. The observed  $M1$  nature of the 784.1-(see Fig. 3), 944.0-keV with  $R_{DCO}$  values 0.64 (5), 0.73 (5), respectively, and 1057.0-keV transitions (refer to [9]), also supports band 2 as the unfavored signature partner band of the  $n_\omega = 0$  phonon band.

Recently, the  $^{125}\text{Xe}$  nucleus was investigated together with the other odd- $A$  Xe isotopes within the framework of the triaxial projected shell model (TPSM) by Jehangir *et al.* [8]. The calculation reproduces the energy levels of the yrast and yrare bands in the various isotopes [8]. In these calculations, the bases space was expanded to include three-neutron configurations as well as configurations based on the coupling of three neutrons with two protons. This was helpful in explaining the high-spin band structures of these odd-neutron Xe isotopes. The adopted value of the axial deformation parameter ( $\epsilon$ ), along with the  $\gamma$  value from the TPSM for  $^{125}\text{Xe}$ , is given in Table I of Ref. [8]. Here, the wobbling energies were

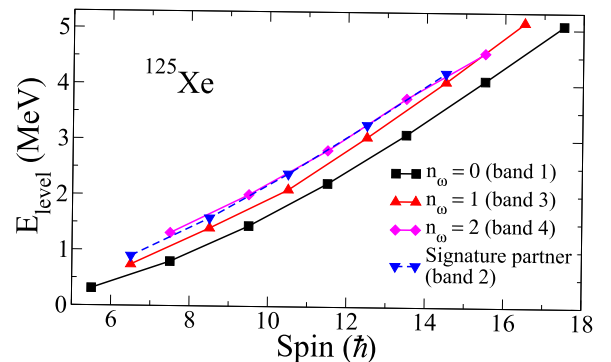


FIG. 8. Excitation energies as a function of spin of bands 1, 2, 3, and 4 in  $^{125}\text{Xe}$ .

calculated by using the proposed theoretical level scheme of  $^{125}\text{Xe}$ , based on TPSM model, and this agrees well with the experimental results (see the comparison between the observed and calculated results in Fig. 7).

On the other hand, the mean value of the rate of change of wobbling frequency ( $|\Delta\hbar\omega_{\text{wobb}}/\Delta I|$ ) as a function of the  $R_E$  values of the core nuclei has been plotted for the  $n_\omega = 1$  wobbling band in Ref. [36]. It is observed that the value of  $|\Delta\hbar\omega_{\text{wobb}}/\Delta I|$  is the largest in  $^{139}\text{Pm}$  ( $\gamma = 28^\circ$ ) with  $R_E \approx 2.5$  [22]. However, the value of  $\Delta\hbar\omega_{\text{wobb}}/\Delta I$  decreases monotonically with  $R_E$  deviating from the value of 2.5. The observed value of  $\Delta\hbar\omega_{\text{wobb}}/\Delta I$  for  $^{125}\text{Xe}$  (calculated by considering  $^{124}\text{Xe}$  as the core nucleus) attains an intermediate value (35.84 keV/ $\hbar$ ) between those of  $^{135}\text{Pm}$  ( $\gamma = 28^\circ$ ) and  $^{133}\text{La}$  ( $\gamma = 26^\circ$ ) [15]. Therefore,  $^{125}\text{Xe}$  appears to be stabilized with a triaxial deformation of  $\gamma = 27^\circ$  (according to the TPSM calculation). Thus, this nucleus shows properties of longitudinal wobbling and this observation of wobbling in  $^{125}\text{Xe}$  further strengthens the suggested correlation between wobbling motion and  $R_E$  or  $Q_0$ , as claimed by Chakraborty *et al.* [26].

#### IV. CONCLUSION

In the present work, directional correlation ratios and angular distributions of transitions in the negative-parity bands (bands 1, 2, 3, and 4) in  $^{125}\text{Xe}$  were extensively studied. Based on the findings presented in this paper, it is concluded that the set of four negative-parity bands originates from the coupling of a  $h_{11/2}$  quasineutron with the ground state configuration of the even-even core. This coupling phenomenon drives the

nucleus towards longitudinal wobbling motion and bands 1, 3, and 4 correspond to  $n_\omega = 0, 1,$  and  $2$  wobbling phonons, respectively. On the basis of large  $M1$  admixtures and the higher excitation energy, band 2 is then identified as the unfavored signature partner of band 1. The mixing ratios, comparatively large  $E2$  fractions, and transition probability ratios are in good agreement with the expected wobbling dynamics. The observed results are found to be in agreement with the recently published calculations within the TPSM model.

#### ACKNOWLEDGMENTS

The authors thank the ANL operations staff at Gammasphere and, in particular, J.P. Greene for help in the target preparation. M.P. acknowledges the fellowship support from the Department of Science and Technology (No. DST/INSPIRE fellowship/2019/IF190275). S.N. acknowledges the financial support from the SERB-DST India under CRG (File No.: CRG/2021/006671). M.P. would also like to thank S. Bhattacharya for his support and valuable advice. The help received from R. M. Clark, P. Fallon, T. L. Khoo, T. Lauritsen, F. Camera, P. Bringel, and C. Engelhardt in this work is gratefully acknowledged. This work is supported by the German BMBF (06 BN 109), the Alexander von Humboldt foundation, Germany, the Danish FNU Council for Natural Sciences, the US Department of Energy, Office of Science, Office of Nuclear Physics, under Contracts No. DE-AC02-06CH11357 (ANL) and DE-AC02-05CH11231 (LBNL), and Grants No. DE-FG02-97ER41041 (UNC), DE-FG02-97ER41033 (TUNL), and DE-FG02-94ER40848 (UML).

- 
- [1] A. Bohr and B. R. Mottelson, *Nuclear Structure* (Benjamin, New York, 1975), Vol. II.
- [2] S. Frauendorf and J. Meng, *Nucl. Phys. A* **617**, 131 (1997).
- [3] S. Frauendorf and F. Dönau, *Phys. Rev. C* **89**, 014322 (2014).
- [4] A. S. Davydov and G. F. Filippov, *J. Exp. Theor. Phys.* **35**, 440 (1958).
- [5] N. Sensharma, U. Garg, Q. B. Chen, S. Frauendorf, D. P. Burdette *et al.*, *Phys. Rev. Lett.* **124**, 052501 (2020).
- [6] R. Wyss, J. Nyberg, A. Johnson, R. Bengtsson, and W. Nazarewicz, *Phys. Lett. B* **215**, 211 (1988).
- [7] R. Bengtsson and S. Frauendorf, *Nucl. Phys. A* **327**, 139 (1979).
- [8] S. Jehangir, Nazira Nazir, G. H. Bhat, J. A. Sheikh, N. Rather, S. Chakraborty, and R. Palit, *Phys. Rev. C* **105**, 054310 (2022), and references therein.
- [9] C.-B. Moon, C. S. Lee, T. Komatsubara, Y. Sasaki, and K. Furuno, *Phys. Rev. C* **76**, 067301 (2007).
- [10] See Supplemental Material at <http://link.aps.org/supplemental/10.1103/PhysRevC.109.034301> for initial level energies ( $E_i$ ),  $\gamma$ -ray energies ( $E_\gamma$ ), spins of initial levels ( $I_i$ ) and final levels ( $I_f$ ), and relative intensities of  $\gamma$  transitions ( $I_\gamma$ ) in  $^{125}\text{Xe}$ .
- [11] A. Gelberg, D. Lieberz, P. von Brentano, I. Ragnarsson, P. B. Semmes, and I. Wiedenhöver, *Nucl. Phys. A* **557**, 439 (1993).
- [12] S. Chakraborty and S. Bhattacharyya, *Proceedings of the DAE Symposium on Nuclear Physics* 66 (2022), and references therein.
- [13] I. Hamamoto, *Nucl. Phys. A* **520**, c297 (1990).
- [14] S. Chakraborty *et al.*, *Phys. Lett. B* **811**, 135854 (2020).
- [15] S. Biswas *et al.*, *Eur. Phys. J. A* **55**, 159 (2019).
- [16] S. Nandi *et al.*, *Phys. Rev. Lett.* **125**, 132501 (2020).
- [17] K. Rojeeta Devi *et al.*, *Phys. Lett. B* **823**, 136756 (2021).
- [18] P. Bringel *et al.*, *Eur. Phys. J. A* **24**, 167 (2005).
- [19] S. W. Ødegård *et al.*, *Phys. Rev. Lett.* **86**, 5866 (2001).
- [20] G. Schönwaßer *et al.*, *Phys. Lett. B* **552**, 9 (2003).
- [21] H. Amro *et al.*, *Phys. Lett. B* **553**, 197 (2003).
- [22] J. T. Matta *et al.*, *Phys. Rev. Lett.* **114**, 082501 (2015).
- [23] N. Sensharma *et al.*, *Phys. Lett. B* **792**, 170 (2019).
- [24] J. Timár *et al.*, *Phys. Rev. Lett.* **122**, 062501 (2019).
- [25] E. A. Lawrie, O. Shirinda, and C. M. Petrache, *Phys. Rev. C* **101**, 034306 (2020).
- [26] S. Chakraborty *et al.*, *Phys. Rev. C* **107**, 064318 (2023).
- [27] R. F. Casten, *Nat. Phys.* **2**, 811 (2006).
- [28] A. Al-Khatib *et al.*, *Phys. Rev. C* **83**, 024306 (2011).
- [29] C. Rønn Hansen *et al.*, *Phys. Rev. C* **76**, 034311 (2007).
- [30] <http://www-gam.lbl.gov>.
- [31] D. C. Radford, *Nucl. Instrum. Methods Phys. Res. A* **361**, 297 (1995).
- [32] A. Granderath *et al.*, *Nucl. Phys. A* **524**, 153 (1991).
- [33] I. Wiedenhöver *et al.*, *Nucl. Phys. A* **582**, 77 (1995).
- [34] E. S. Macias, W. D. Ruhter, D. C. Camp, and R. G. Lanier, *Comput. Phys. Commun.* **11**, 75 (1976).
- [35] D. R. Jensen *et al.*, *Phys. Rev. Lett.* **89**, 142503 (2002).
- [36] S. Rajbanshi *et al.*, (private communication).